Global Scientific JOURNALS

GSJ: Volume 8, Issue 8, August 2020, Online: ISSN 2320-9186
www.globalscientificjournal.com

Analyze Fatigue Behavior of Wheel-Rail under Rolling Contact Loading Condition Using Finite Element Method

[1]Aregawi Hailemariam, [2]Negash Alemu, [3]Amberbir Wondimu

[1] Department of Production, Defense University (DU), Bishoftu, Ethiopia,

[2] Department of Metallurgical & Materials Engineering, Defense University (DU),

Bishoftu, Ethiopia,

[3]Department of Mechanical Engineering, Haramaya Institute of Technology, Haramaya University, Harar Ethiopia

ABSTRACT

The main purpose of this article is to analyze fatigue strength of wheel-rail under design and the influence of maximum axle load.

In this article, the analysis is done under two loading of conditions (i.e., design load and the worst loading scenario).

Under these two loading conditions, the various contact fatigue stresses, maximum contact pressure are evaluated at the wheel -rail interface and wheel, rail separately.

FEM is used to determine the contact fatigue stresses and maximum pressure. The wheel-rail assembly is modeled in CATIA V5 R19 there after it is imported as an IGS file format into ANSYS workbench software.

Extensive review of books, field survey, published journals have carried out to achieve the study.

From the analysis, it is found that in both loading situations, the highest equivalent stress is found at the rail section. The outcomes of this work is believed to be useful in rolling fatigue design in the academic community and railway industry at large in terms of providing insight in fatigue design of wheel-rail . Furthermore, it can greatly assist the society to ensure their safety and well-being.

Key words: Rolling contact fatigue, FEM, Hertz contact theory

1. INTRODUCTION

In recent years with the continuous increase of the axle load, the influence of the contact forces on the wheel-rail damage has received more and more attention. With view of this demand for transporting of commodities and passengers in Addis Ababa, which is being increasing from day to day in the city. Here in Addis Ababa it is familiar to see long lines during the peak time. As shown in figure 1.1 during these peak times, the trains have been travelling by carrying beyond the intended standard design load. This means of transportation is almost new technology to Addis Ababa city that provides transportation service for 200 thousand persons per day via 41 vehicles.

Figure 1.1 Taxi queue in Addis Ababa

As many evidences in the area of fatigue witnessed that rolling contact fatigue(RCF) is a problem that knows no borders [1].

Taek-Young et.al.[2] presented three-dimensional elastic–plastic stress analysis of rolling contact of railway wheel is conducted on a 3D wheel-rail model. Then, the contact pressure distributions calculated using elastic Hertz theory and three-dimensional elastic–plastic stress analysis were compared.

Roya Sadat et.al. [3] has investigated the maximum contact stresses in the contact area of the wheel and rail as a result of lateral movement of the wheel on rail by taking advantage from Hertz theory. The total load on each wheel considered was 63.75 KN. From the investigation, the

maximum contact pressure was found 1603.84 Mpa.

The current study focuses methodology to estimate the wheel-rail, contact fatigue stress analysis under design and maximum axle load conditions via finite element approach. The design load has assumed six persons/m^2 while the maximum load has considered eight persons/ m^2.On top of considering eight persons/ m^2; this study has taken in to account parameters like speed and wheel-rail irregularity.

Furthermore, design of Addis Ababa light rail transit (AALRT) services is based on the assumption of static load, considering 63.2 ton of overload capacity and additional 3 % of the overload capacity consideration. It does consider dynamic assumption. Journals like [4, 5] affirms this fact.

2. The Normal Problem (Hertz theory):

These Contact problems are analyzed based on the Hertz theory. In 1882, Hertz published his theory on the contact between elastic bodies [6].

The main assumptions of the theory are as follows:

- The material of the bodies is elastic. The two bodies may each have a different set of material properties.
- The strains are small and within elastic limit
- The contact area is small compared to the local curvature of the contacting bodies.
- The curvatures are constant inside the contact patch.
- Smooth surfaces where the surface roughness is neglected

The normal force of contact between two contacting surfaces, their longitudinal and transverse radii of curvature, and the elastic properties of each of the bodies in contact are required in the form of input data for the calculation of the contact patch parameters.

The onset of yield in sliding contact, or combined rolling and sliding, as between wheel-rail contact width $a,\ b$ and pressure distribution p(x) are given by Hertz equation [6] as,

$$P(x,y)=\frac{3F_z}{2\pi ab}\sqrt{1-\frac{x^2}{a^2}-\frac{y^2}{b^2}} \qquad (2.1)$$

$$-a \le x \le a \text{ and}$$

$$-b \le x \le b$$

Where a and b are the contact patches in the longitudinal and in the lateral direction respectively.

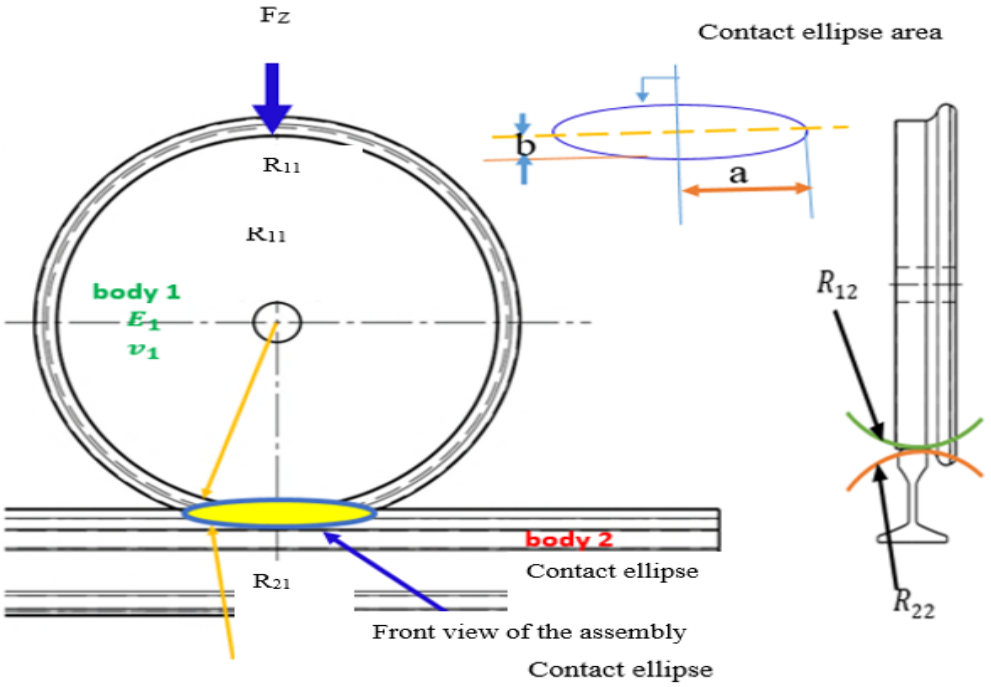

Figure 2.1 Contact surface between wheel-rail

2.1. Wheel-Rail Rolling Contact and Effects Dynamic Load

For a static axle or wheel load, the dynamic load $F_v(dyn)$ can be modelled as a statistical distribution, the upper bound of which can be used as worst condition for design purposes. This is realized by multiplying the static load with a magnification factor K_{dyn} as [8] .

$$K(dyn) = 1 + 3.n.\varphi \tag{2.2}$$

With n=0.15 to 0.25 for different types of tracks

Where n=rail irregularity parameter

φ =speed parameter

$$\varphi = \begin{cases} 1 \; for \; V \le 60 \, {}^{km}/_{h} \\ 1 + 0.5(V - 60)/190 \; for \; V \; 60 \le V \le 300 \, {}^{km}/_{h} \; (passenger \; train) \\ 1 + 0.5(V - 60)/80 \; for \; V \; 60 \le V \le 140 \, {}^{km}/_{h} \; (freight \; train) \end{cases} \tag{2.3}$$

$$F_v(dyn) = F_n \times K(dyn) \tag{2.4}$$

The contact stresses and pressure increases with increasing of irregularities of wheel-rail such as corrugation of rails or flat spots on the wheels especially at high speeds.

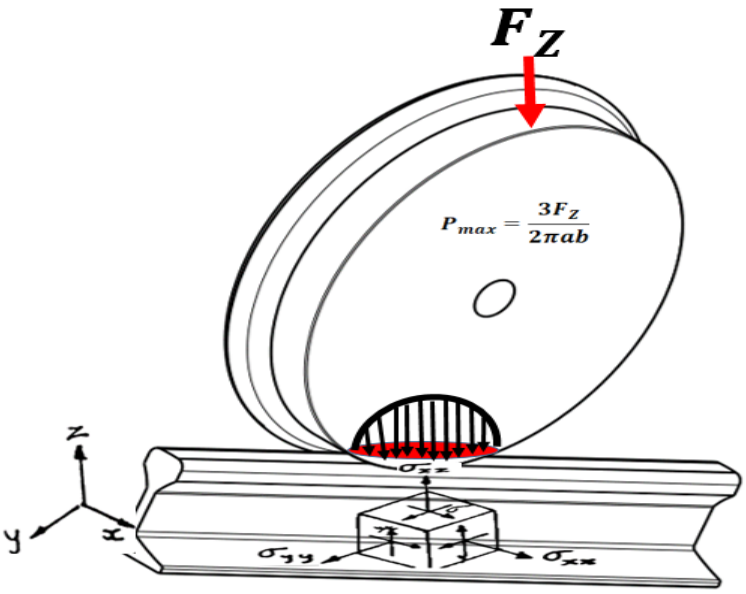

Figure 2.2. 3D Contact stress tensor representation at the contact area.

The following data are collected from AALRT as shown in Table 2.2 and 2.3.

Table 2.1 Rated passenger capacity of vehicles

Number of passengers (persons)	Seated	Standing	Total
Seats (AW1)	65	0	65
Rated passenger capacity (AW2) (standing: 6 persons/m^2)	65	189	254
Overload capacity (AW3) (standing: 8 persons/m^2)	65	252	317
Empty vehicle (t)	44	0	44
Rated passenger capacity (t)	44	15.24	59.24
Overload capacity (t)	44	19.02	63.02

Table 2.2 miscellaneous specifications

R/No	Description	Load
1	The maximum operating speed of vehicle	70 km/h
2	The minimum operating speed of vehicle	20 km/h
3	Average weight of a passenger	60 kg
4	Number of axels	6
5	Number of wheels	12
6	Wheel diameter	840 mm
7	Sleeper spacing	625 mm
8	Length of car body	≤30000 mm
9	Maximum width of car body:	2650 mm
10	Annual ambient temperature	25.5 ℃
11	R11=the rolling radius of curvature of the wheel	420 mm
12	R12 = the radius of the wheel profile	∞
13	R21= the rail radius of the runway that is infinity for the radius of the rail is straight from the side view.	∞
14	R22=the radius of curvature of the rail in the plane of cross section	300 mm

- **Load Distribution and Conversion**

- ✓ Tram car weight=44 ton=440 quintal=44000kg=431,640N
- ✓ Carrying Capacity=317 person
- ✓ Each person weight=60 kg
- ✓ Total load in (t) =317× 60 = 19.020 t = 186,586.2 N
- ✓ Rated passenger capacity (t) =254× 60=15.04=149,504.4 N
- Total load = Tram car weight+ Carrying Capacity=431,640+186,586.2 = 618,226.2N
- Total design vertical load on each wheel=618,226.2N/ 12=51,518.85N≅51,519 N

2.2. Developing Design Criteria

Von Misses yield criterion is known as the maximum shear strain energy criterion, as

yielding is predicted to occur when the equivalent stress is equal to the yield strength of the material.

Von- Mises criterion can be used to evaluate the strength of element subjected to the action of stresses that cause its distortion. The Von-Mises theory is preferable since it takes into account all three principal stresses.

3. FEM analysis and simulation

The basic theory of finite element method is representation of a body or a structure by an assemblage of small sub-divisions called finite elements. These elements are considered interconnected at joints, which are nodes or nodal points. The elements are superimposed on to a coordinate guided system, where nodal points are preferred with respect to a coordinate system. The position and elastic properties of elements are defined by the matrices, so that the displacement of each element can be related to the forces on the element.

Yield occurs when

$$\sigma_v = \sqrt{\frac{1}{2}\left[\left(\sigma_{xx}-\sigma_{yy}\right)^2+\left(\sigma_{yy}-\sigma_{zz}\right)^2+\left(\sigma_{zz}-\sigma_{xx}\right)^2\right]} \le \sigma_y$$

According to this criterion, plasticity will start when the Von-Mises stress is greater than the yield strength of the material. The maximum contact stress is greater than the expected yielding strength. Therefore, the wheel-rail can initiate plasticity

During the analysis, the following considerations are the recommended practices that ought to be came in to picture while executing the whole study.

1. Modeling the geometry
2. Meshing (discretization)
3. Selection of material property
4. Boundary and loading conditions
5. Developing design criteria
6. Validating with related works

Table 3.1 Mechanical properties of CL60 wheels [11]

Part Name	Young's modulus (Gpa)	Ultimate tensile strength (σ_{ut}) (mpa)	Yield strength (σ_y) (mpa)	Poison ratio	density $\left(kg/m^3\right)$	Maximum deformation %
Wheel	210	1020	665	0.3	7850	15
Rail	207	780	640	0.27	7800	12

3.1. Modeling, boundary and loading conditions

The model is meshed using tetrahedron elements as shown figure 3.1. The mesh and the number of elements used in the FE model have a significant effect on the results obtained and the computational time/cost.

As we select tetrahedral elements, the following computation is taking place briefly in the Ansys black box.

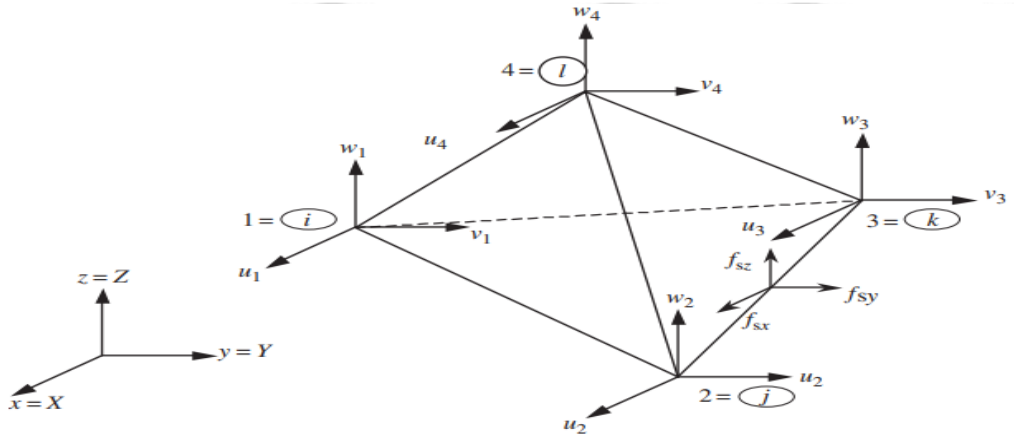

Figure 3.1 Solid block divided into four-node tetrahedron element [11].

$$\varepsilon = LU \qquad (3.1)$$

$$U = \begin{Bmatrix} u \\ v \\ w \end{Bmatrix} \qquad (3.2)$$

The constitutive equation gives the relationship between the stress and strain in the material of a solid by the Hooke's law

$$\sigma = c\varepsilon \qquad (3.3)$$

$$\sigma = CLU = CLNd_e = CBd_e \qquad (3.4)$$

Where B the is strain matrix, d_e the nodal displacement, N shape functions, C is the material constant matrix for isotropic

materials, L is the differential operator for detail please refer [11]

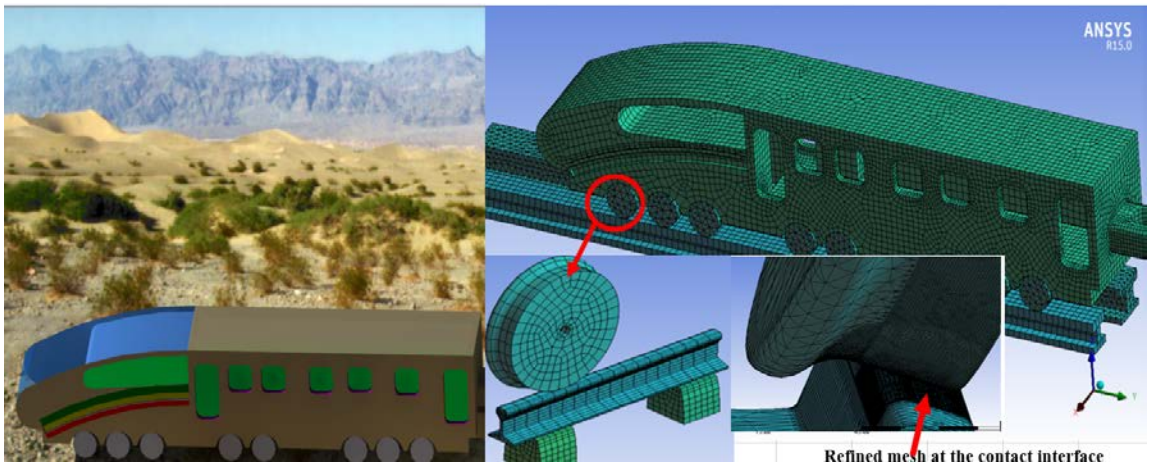

Figure 3.2. **3D** Model and mesh generation.

To achieve accurate result the Ansys default is customized such that the span angle center from coarse to fine, smoothing from low to high, relevance center from coarse to fine have been done. The refinement process was only applied on the local critical regions of the contacting area to avoid the occurrence of stress singularity.

Figure 3.3 shows the element quality in the contact regions of the model. Element quality ranges from 0.15–0.20 is said to be acceptable and above 0.20 is considered good element [11].

In view of this all, the important regions (across the interface) were having an element quality greater than or equal to 0.6 as shown in Figure 3.3.

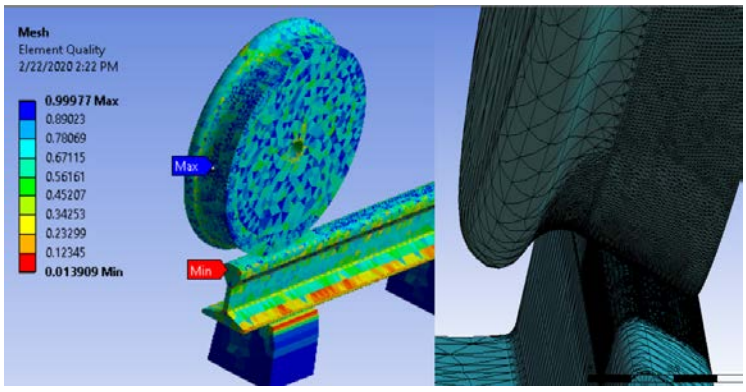

Figure 3.3 Refined meshed wheel- rail assembly

Table 3.2 Mesh results when relevance center, span angle and smoothing is set to fine

Part name	Element type	Element size at the contact in "mm"	Number of element	Number of nodes
Wheel	Linear tetrahedron	2	136014	233705
Rail	Linear tetrahedron	2	73385	125235
Sleeper	Linear tetrahedron	default	1470	2795

The boundary conditions are applied to the bodies in order to restrict undesired displacements of the bodies in the analysis. The boundary conditions are selected according to the coordinate system. For structural DOF constraints are two types (i.e. translational and rotational) these can be labeled as in Ansys as U_x, U_y, U_z translational motion in the X, Y, Z direction and Rot_x, Rot_y, Rot_z rotational motion in the X,Y,Z direction respectively.

In light of this, the bottom of the rail was constrained in all directions. Rolling of the wheel part in the longitudinal directions is set free. Contact 174 and target 170 element are used in Ansys workbench between the contact and target bodies. The reason behind is conta174 is used to represent contact and sliding between 3-D target surfaces. Friction effect is included into the material properties of the contact element as shown in the figure 3.4.

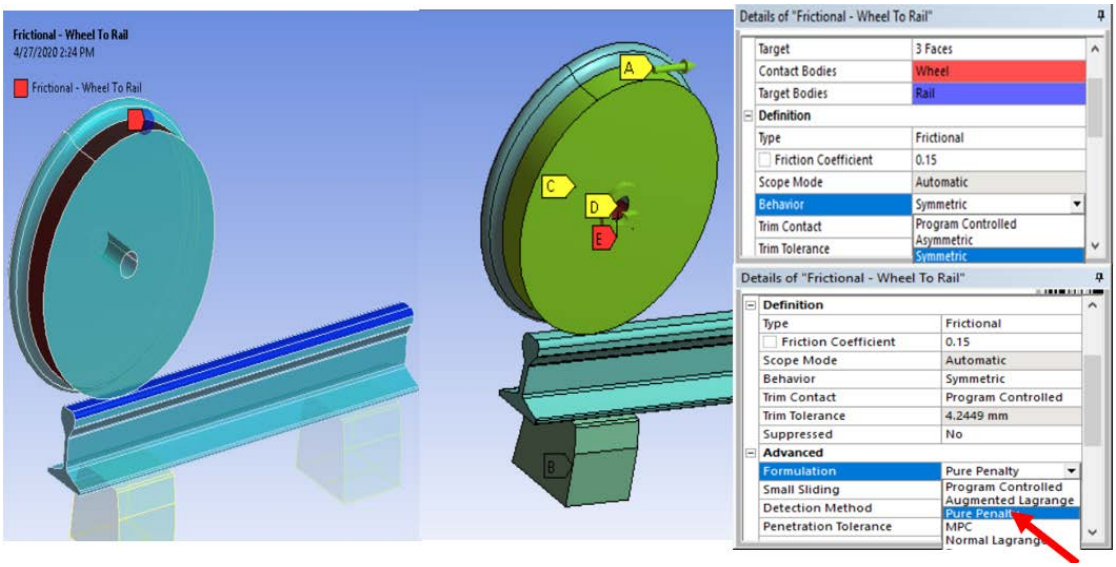

Figure 3.4. Assignment of boundary condition between wheel and rail

4. RESULTS AND DISCUSSIONS

Finally, FE model is run and post-processed successfully to visualize stresses and maximum pressures.

From the static perspective the maximum Von vises stress on the small area of wheel-rail is 348.53 MPa on the wheel and 485.41 MPa on the rail is found as shown in Figure 4.1

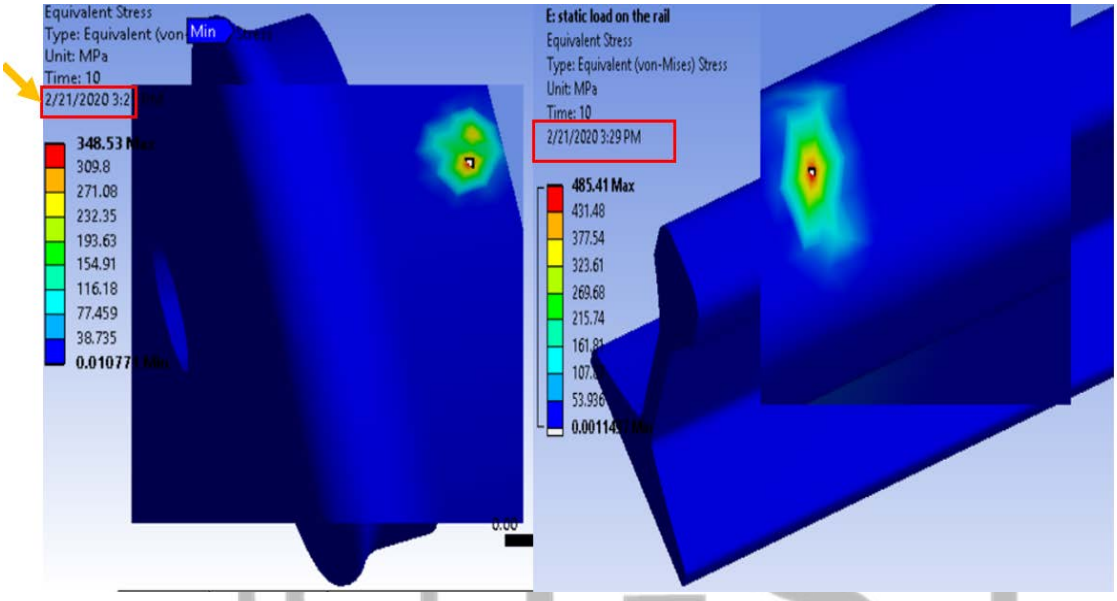

Figure 4.1 Maximum Von vises stress of wheel and rail at the static load

Regarding the dynamic load Von -Mises stress on the wheel and rail independently is 512.11 and 662.33 MPa respectively. This result is depicted in the contour result Figure 4.2.

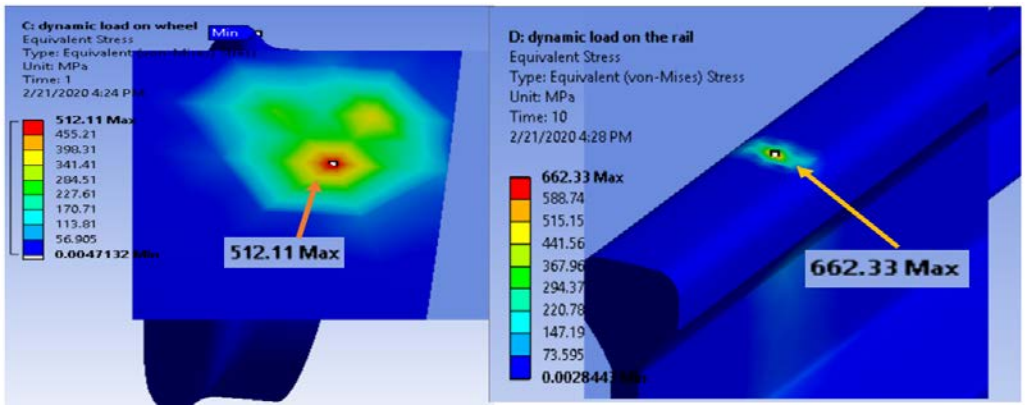

Figure **4.2** wheel-rail Von vises stress result at the dynamic load

Figure 4.3 shows Von-Mises maximum stress contour, maximum pressure due to dynamic, loading. The stresses are concentrated over the small contact area. The maximum stress and pressure at the dynamic load is found 662.33 MPa and 1622.1 MPa respectively.

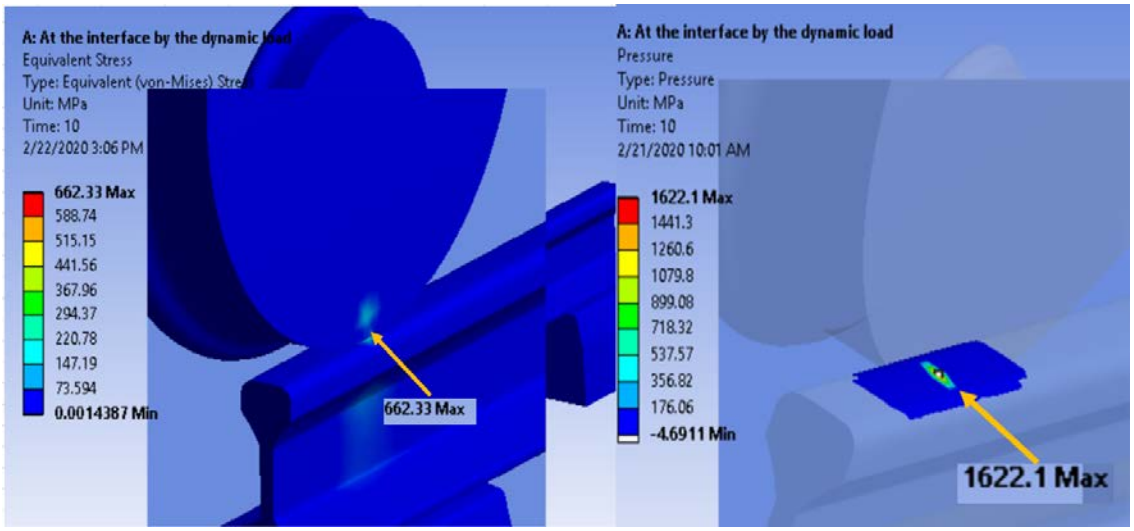

Figure **4.3**equivalent stress and pressure result induced on the wheel-rail contact region

Figure 4.4 represents the stress and the maximum pressure at the design load. The stress and maximum pressure result obtained was 370.31 and 893.84 MPa respectively.

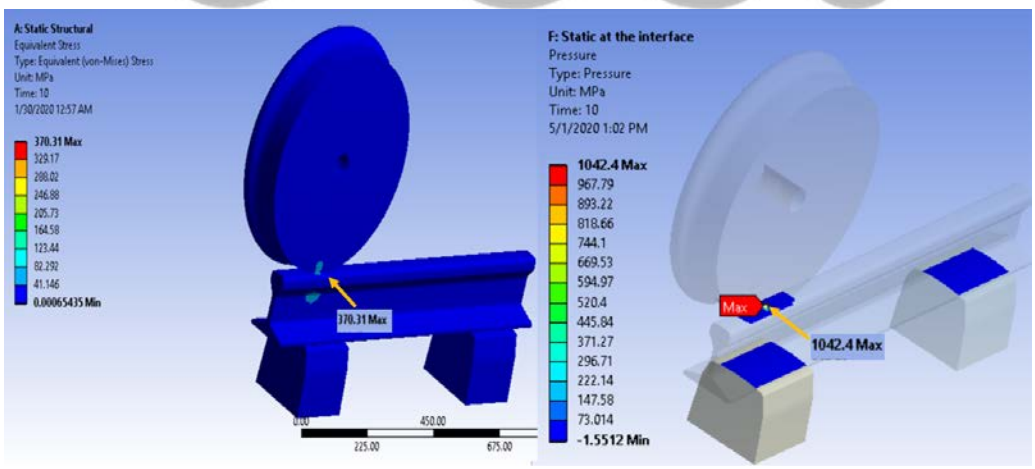

Figure 4.4 equivalent stress and pressure result induced on the wheel-rail at the dynamic load

While dealing separately for the wheel and the rail the maximum stress at the contact region is transferred to the rail part as show in Figure 4.5.

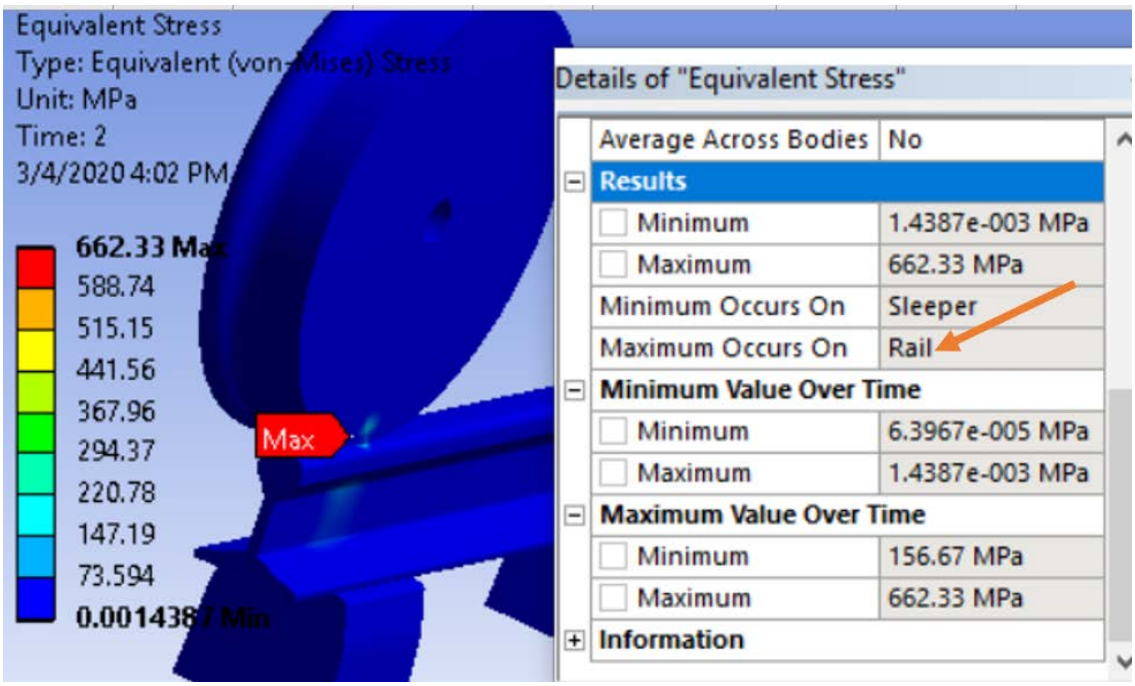

Figure 4.5 Indication of maximum stress over time

Figure 4.6 below shows the level of stress over time. From the time at 0.9125 seconds, the equivalent stress is 632.65 MPa and at exactly one sec, the equivalent stress is 662.33 MPa. Right after one second from Figure 4.6 shown, it is clear evidence that the stress is constant and converged.

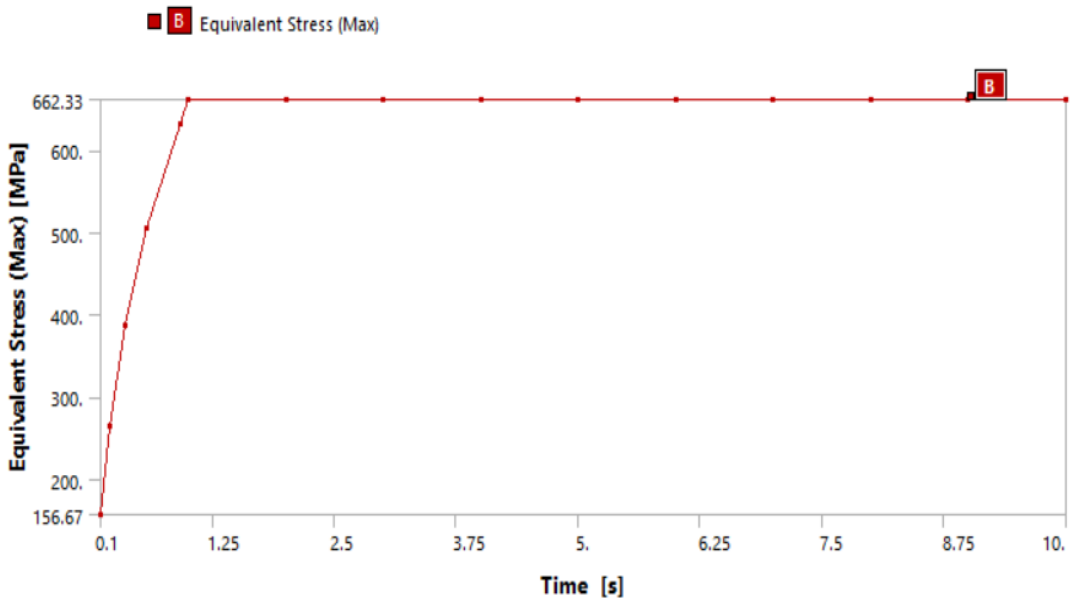

Figure 4.6 Relationship between equivalent stress and time

Figure 4.7 below shows the maximum strain is found 0.00313 mm when the stress is highest at the worst load condition.

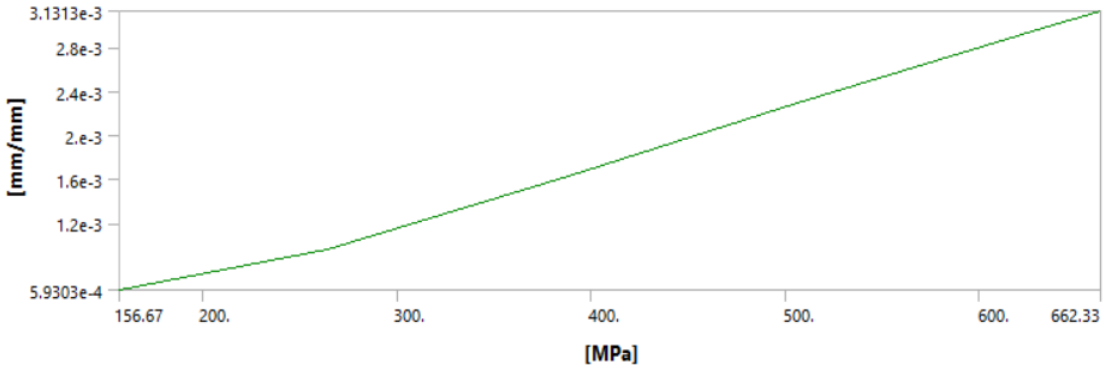

Figure 4.7 Relationship between equivalent stress and total strain plot

In Table 4.1, a comparison is made between the FEM and the analytical method. According to this table, it is obvious that the

FEM is less than from the analytical method. This discrepancy is due to

- Assumption of elastic property in the Hertz theory
- Assumption of elastic-plastic in the FEM
- More realistic contact is created between wheel-rail in the FE than Hertz

4.1. Conclusion

Plasticity is initiated by von-misses design criteria at the maximum load while it was found that safe in the design load.

From the investigation, it is found that the maximum and minimum equivalent stress is obtained at the rail and wheel respectively. From the above numerical data, it is found that the rail is weaker than the wheel.

That is due to either of the following reasons:

- ✓ The wheel material strength is greater than the rail
- ✓ The rail is suspending between two sleepers thereby it could stagger by the high pressure of the wheel load
- ✓ There are stress risers on the railhead and web connections thus this portion is prone to high stress.
- ✓ From the Equivalent (von-Mises) Stress design criteria perspective, the maximum equivalent Stress (Von-Mises stress) is lower than the yield strength of the wheel material. This reveals that the stress level at the contact region does not threaten to failure.
- ✓ From the Von-Mises stress design criteria, the equivalent stress is greater than the yield strength of the rail, which tells us plasticity will, initiated because of the high stress at this region.

4.2. Recommendations

The following suggestion or recommendation can be drawn from the knowledge gained;

- Predictive and preventive maintenance will help to increase safety and wellbeing of the passengers.
- Preventive maintenance, activities carried out before breakdown occurs, includes such as inspection, detection and corrective actions should be implemented.

- Experimental investigation would have to be carried out in order to confirm the theoretical result.
- Establishment of regular inspections and appropriate maintenance strategy are the crucial advice that would implemented by institution.

Acknowledgement

This research was supported by defense University College of engineering. We thank our colleagues from defense University College of engineering, who provided scientific insight and expertise advice that greatly assisted the research. I gratefully thanked for Addis Ababa light rail transit service management bodies for the cooperation they made.

Disclosure statement

The authors reported no potential conflict of interest.

Funding

This research was supported by Federal Democratic republic of Ethiopia Ministry of defense.

References

[1] E. E. Magel, "Rolling Contact Fatigue: A Comprehensive Review," *Fed. Railr. Adm.*, no. November, p. 132, 2011, doi: 10.1039/B910216G.

[2] T. Kim and H. Kim, "Three-dimensional elastic-plastic finite element analysis for wheel-rail rolling contact fatigue," vol. 6, no. 3, pp. 1593–1600, 2014.

[3] R. S. Ashofteh, "Calculating the Contact Stress Resulting from Lateral Movement of the Wheel on Rail by Applying Hertz Theory," vol. 6, no. 4, pp. 148–154, 2013.

[4] S. Guta and D. Tilahun, "Stress Analysis of Rail Joint under Wheel Load," vol. 3, no. 6, pp. 526–543, 2016.

[5] China Railway Group Limited, "Technical Specifications of Vehicles," no. July, pp. 1–116, 2013.

[6] M. Buddhe, "Analysis of rail-wheel contact stresses using finite element method in comparison with analytical solution," vol. 3, no. 8, pp. 31–37, 2016.

[7] U. Zerbst, M. Katrin, and H. Hintze, "Fracture mechanics in railway applications — an overview," vol. 72, pp. 163–194, 2005, doi: 10.1016/j.engfracmech.2003.11.010.

[8] U. Zerbst, R. Lundén, K. Edel, and R. A. Smith, "Introduction to the damage tolerance behaviour of railway rails – a review," *Eng. Fract. Mech.*, vol. 76, no. 17, pp. 2563–2601, 2009, doi: 10.1016/j.engfracmech.2009.09.003.

[9] M. Zhang and H. Gu, "Microstructure and mechanical properties of railway wheels manufactured with low-medium carbon Si-Mn-Mo-V steel," *J. Univ. Sci. Technol. Beijing Miner. Metall. Mater. (Eng Ed)*, vol. 15, no. 2, pp. 125–131, 2008, doi: 10.1016/S1005-8850(08)60025-0.

[10] G. R. L. and S.S.Quek, The finite

element method a practical course. Linacre House, Jordan Hill, Oxford OX2 8DP, 2003.

[11] A. Wondimu, N. Alemu, Y. Regassa, and P. Sivaprakasam, “Modelling and simulation of effect of missed bolt on rail end joint by fem,” *Int. J. Ambient Energy*, vol. 0, no. 0, pp. 1–8, 2020, doi: 10.1080/01430750.2019.1707115.